

A first principles study of magnetism in Pd₃Fe under pressure

Biswanath Dutta,¹ Sumanta Bhandary,² Subhradip Ghosh,¹ and Biplab Sanyal^{2,*}

¹*Department of Physics, Indian Institute of Technology Guwahati, Guwahati, Assam 781039, India*

²*Department of Physics and Astronomy, Uppsala University, Box-516, SE 75120, Uppsala, Sweden*
(Dated: October 3, 2012)

Recent experiments on Pd₃Fe intermetallics [Phys. Rev. Lett. 102, 237202 (2009)] have revealed that the system behaves like a classical invar alloy under high pressure. The experimental pressure-volume relation suggests an anomalous volume collapse and a substantial increase in bulk modulus around the pressure where invar behavior is observed. With the help of first-principles density functional theory based calculations, we have explored various magnetic phases (ferromagnetic, fully and partially disordered local moment, spin spiral) in order to understand the effect of pressure on magnetism. Our calculations reveal that the system does not undergo a transition from a ferromagnetic to a spin-disordered state as was thought to be the possible mechanism to explain the invar behavior of this system. We rather suggest that the anomaly in the system could possibly be due to the transition from a collinear state to non-collinear magnetic states upon the application of pressure.

PACS numbers: 63.20.dk, 63.50.Gh

I. INTRODUCTION

The technological usefulness of the state-of-the-art magnetic materials depends on their properties at finite temperature and pressure. Fe-based alloys and intermetallics have their rich history of being used as smart magnetic materials¹. Numerous experimental and theoretical investigations have been carried out to understand the magnetic properties of pure Fe and its alloys and intermetallics at finite temperatures²⁻⁴ (and references therein). A very special characteristic of some Fe-based alloys is observed as the invar properties where the thermal expansion coefficient remains invariant with temperature. A wealth of literature on theoretical and experimental results on invar alloys exist.²⁻¹⁰ Besides the conventional temperature invariant invar properties, pressure induced invar characteristics have also been reported.¹¹

In this paper, we will discuss an Fe-based alloy where pressure induced invar properties have been observed in experiments recently.¹² EDXAD experiments on Pd₃Fe alloys have reported an anomalous volume collapse under pressure between 10 and 15 GPa¹². The EDXAD data were successfully fit to a equation of state which points towards the existence of two separate states; one at high pressure and the other at low pressure. Subsequent measurements at high temperatures reveal that at 7 GPa pressure, there is an anomalously low thermal expansion suggesting that the system behaves like an Invar alloy⁶ at high pressure. First principles calculations to understand the origin of these anomalies were rather inconclusive. However, in order to explain the invar behavior under pressure in this system, it was conjectured that the application of pressure may reduce the Curie temperature below room temperature, thus making possible a transition in magnetic state from ferromagnetic to a spin-disordered one and that the invar anomaly is a result of such high volume-high spin to low volume-low

spin transition¹². Such a proposition stems from the facts that in Fe-rich FePt and FePd alloys, the classical invar anomaly at ambient pressure was explained in terms of the transition from a high volume ferromagnetic state to a low volume spin disordered state⁷⁻⁹. In case of Fe-based alloys with low Fe concentration, the magnetically ordered state was found to be stabilized and thermal invar behavior was suppressed, in general. However, it was discovered that in case of Fe-Ni alloys with low Fe concentration, the alloy with normal thermal expansion properties at ambient pressure exhibits invar behavior at high pressure¹¹. This explanation for this anomaly was given in terms of transition to non-collinear configurations at lower volumes due to application of pressure. On the other hand, Khmelevsky *et al.*¹³ investigated the magnetic transitions in Fe_{0.7}Pt_{0.3} under pressure and ruled out the possibility of making a connection between the observed invar anomaly and a transition to noncollinear states from zero pressure collinear one. These results, thus, indicate that the physical origin of anomalies related to the magnetic properties in Fe-based alloys under pressure may not be unique. In this paper, we, therefore, aim at understanding the magnetism in Pd₃Fe alloys under pressure by extensive quantitative analysis of the energetics, the magnetization, the pressure-volume relations with different magnetic structures. To this end we have performed first principles calculations with the collinear magnetic structures viz. ferromagnetic, antiferromagnetic, and the spin disordered structures and with the spiral magnetic structures. Our results show that contrary to the proposition in Ref. 12, the volume collapse and the subsequent invar anomaly under pressure, observed experimentally, cannot be explained by a transition from magnetically ordered state to a spin disordered state. Rather, the results indicate that the anomaly could be due to the transition from a collinear magnetic state to noncollinear ones.

The paper is organized as follows. In Section II, we

briefly discuss the details of computational methods used. In Section III, we present our results on various magnetic structures. A detailed discussion followed by the conclusions are presented at the end.

II. COMPUTATIONAL DETAILS

All calculations have been performed within the standard framework of the spin polarized version of the density functional theory^{14,15}. The spin disordered magnetic structure has been simulated using the disordered local moment (DLM) formalism¹⁶ where the magnetic disorder is represented by considering the Pd_3Fe system as a pseudoternary alloy $\text{Pd}_3\text{Fe}_x^+\text{Fe}_{1-x}^-$, where x is the concentration of Fe atoms with up spin (Fe^+) and $1-x$ is with down spin (Fe^-). The paramagnetic or the full DLM state, henceforth mentioned as FDLM, is obtained when $x = 0.5$. Partial disordered local moment (PDLM) is realized for $x \neq 0.5$. Calculations for the DLM states are performed by the Green's function based Exact Muffin-tin Orbital (EMTO)¹⁷⁻¹⁹ formalism in conjunction with the Coherent Potential Approximation (CPA)²⁰, a single site mean field formalism to treat the chemical and magnetic disorder. The EMTO-CPA is a suitable method for the treatment of the spin disordered state as the usage of conventional electronic structure methods require construction of prohibitively large supercell to simulate the magnetically disordered states. The other advantage of the EMTO method is that it uses two different approaches for calculations of the one-electron states and the potentials: while the one electron states are calculated exactly for the overlapping muffin-tin potentials, the solution of the Poisson's equation can include certain shape approximations. An accuracy at a level comparable to the full-potential techniques can, thus, be sustained, without a significant loss of accuracy. However, since the present implementation of the EMTO method does not address noncollinear magnetic ordering, the spiral magnetic structures have been studied by the full-potential linearized augmented plane wave (FP-LAPW) method²¹ using the ELK code²² in an implementation which allows noncollinear magnetism including spin spirals^{23,24}. In this implementation, the full magnetization density is used in addition to the full charge density and the full potential. The magnetic moment is allowed to vary both in magnitude and in direction inside the atomic spheres as well as in the interstitial regions.

All calculations have been performed within the local spin density approximation (LSDA)²⁵ for the exchange-correlation part of the Hamiltonian. For the EMTO-CPA calculations, the Green's functions were calculated for 32 complex energy points distributed exponentially on a semi-circular contour. The total energies were calculated by the full charge density technique²⁶. The s , p and d orbitals were included in the EMTO basis set for the expansion of the wave functions. The Brillouin zone integrations were performed with 1540 \mathbf{k} -points. In the

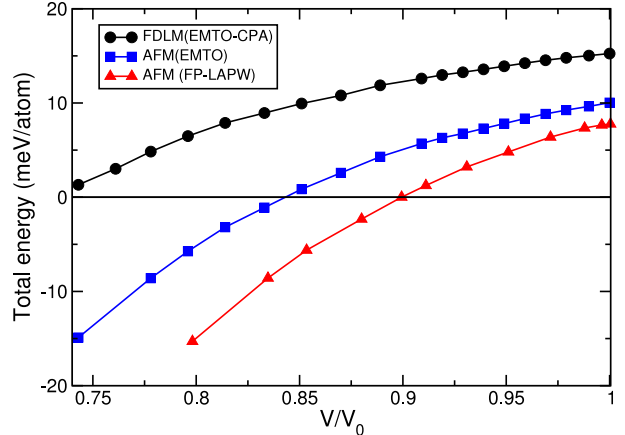


FIG. 1. (Color online) Total energy as a function of V_{red} for FM, AFM and DLM states computed by the EMTO-CPA method. The energy of the ferromagnetic state is taken to be zero. The results of FP-LAPW calculations for FM and AFM states are shown for comparison.

FP-LAPW method, the muffin tin radii of Fe and Pd were taken to be 1.16 and 1.27 Å respectively. The plane wave cutoff for basis functions is $RK_{max} = 8$. The cutoff for the charge density was considered to be $G_{max}=12$. The number of \mathbf{k} -points for the Brillouin zone integrations were 364. A broadening of 0.14 eV was used according to Methfessel-Paxton²⁷scheme. Total energies were converged to less than 1 meV per atom for all the calculations.

III. RESULTS AND DISCUSSIONS

In Ref. 12, pressure-volume relations for Pd_3Fe showed an anomalous reduction in volume from $V_{red} = \frac{V}{V_0} = 0.96$ to 0.91 between 10 and 15 GPa pressures, V_0 being the equilibrium volume of the ferromagnetic state. Since the pressure-volume curve could be smoothly fitted to a Weiss like equation of state, it was proposed that the anomaly is related to the transition from a high volume-high spin state to a low volume-low spin state. On the other hand, the low thermal expansion under pressure suggested an invar anomaly and its connection to the two state model of Weiss²⁸. The authors, however, could not find out a stable low spin state at lower volume from first-principles calculations. Therefore it was proposed that the required low volume-low spin state could be a paramagnetic state. Such a transition, according to them, could be because of lowering of the Curie temperature T_c due to the application of pressure. In this section, we present results of extensive first-principles calculations to resolve these issues.

In Fig. 1, we present results on the relative stabilities of

ferromagnetic (FM), antiferromagnetic (AFM) and paramagnetic (PM) states by EMT0, EMT0-CPA and FP-LAPW methods. PM state has been modeled by a full disordered local moment (FDLM) treatment. The AFM state, considered for comparison, has Fe moments ordering ferromagnetically in alternating (110) planes. We have done calculations for two other AFM states, in one of which the Fe moments order ferromagnetically in alternating (100) planes and in the other in alternating (111) planes. The energy of the first one, the (110) AFM was the lowest and hence it has been included for comparison. The results of the EMT0 and EMT0-CPA calculations show that the AFM state becomes stable in comparison to the FM state at $V_{red} \sim 0.85$, while the DLM state would be stable at a much higher compression. The FP-LAPW calculations predict that the AFM state becomes stable at $V_{red} = 0.9$. It is to be noted that the first-principles projector augmented wave calculations of Ref. 12 also observed stabilization of the AFM state at around $V_{red} = 0.9$. The proximity of the FP-LAPW and the projector augmented wave results are not surprising since both solve the Kohn-Sham equations without invoking any shape approximations on the charge density and potential. A different V_{red} value for FM-AFM transition as computed by the EMT0 is due to the fact that certain degree of shape approximations is inherent in the muffin-tin orbital based methods. However, this discrepancy does not seriously affect the physics as our primary concern here is to find out a magnetic phase, energetically lower than the FM state at around the experimental pressure where the anomalous behavior in pressure-volume relation is found and relate the stability of the phase with the anomalous behavior. It is to be noted that the V_{red} values of 0.9 obtained by the FP-LAPW or of 0.85 obtained by the EMT0 for the FM-AFM transition are quite close to the V_{red} value of 0.91 where the anomalous volume collapse was observed in EDXD measurements. However, the outcome that the FDLM state is having a energy higher than the FM state until a much larger compression, rules out the proposition of Ref. 12, that the FM state transforms to the paramagnetic state upon compression with a lowering of T_c . In order to validate our argument, we have calculated the T_c as a function of the compression, as shown in Fig. 2. The T_c has been estimated by the mean-field approximation as,

$$k_B T_c = \frac{2}{3} (E_{FDLM} - E_{FM}) \quad (1)$$

where E_{FDLM} , E_{FM} are the total energies of the system in FDLM state and in the ferromagnetic states respectively. The calculated T_c of 472K compares well with the experimental value of 499K²⁹ at zero pressure ($V_{red} = 1$). The results suggest that the T_c indeed decreases with pressure and reduces below room temperature at around $V_{red} = 0.85$. This, though, may tempt one to infer that at this compression, the system should undergo a transition from FM to PM state, making a correlation between this result and the anomalous volume collapse, observed

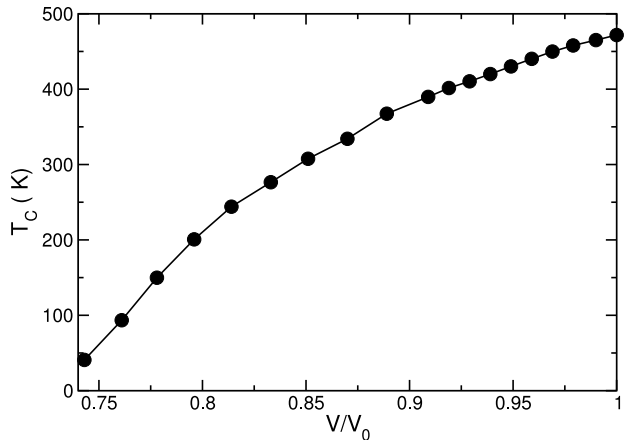


FIG. 2. Curie temperature T_c as a function of V_{red} computed by the EMT0-CPA method.

experimentally, requires two things: first, the zero pressure volume of the PM state should be significantly lower than the FM state, introducing volume magnetostriction as is observed in the FePt and FePd alloys with high Fe concentrations where the invar anomaly is observed⁷ and second, the bulk modulus of the low volume state should be substantially higher than the high volume FM state as was observed experimentally¹². In Table I, we present results on zero pressure lattice constant and bulk modulus computed for the FM, the AFM and the DLM states. Results obtained by the EMT0 and the FP-LAPW methods along with the theoretical results of Ref. 12 are presented for comparison. The results clearly show that the equilibrium lattice constants and the bulk modulus of the FM, AFM and FDLM states calculated by the EMT0-CPA method are nearly equal, thus leaving no scope of observing magnetostriction and the features in bulk modulus observed in experimental data of Ref. 12. The FP-LAPW calculations for FM and AFM states also imply the same trend with regard to these two magnetic states. Another feature of the invar anomaly observed in case of Fe₃Pt alloy was that the low volume FDLM state had significant reduction in the magnetic moment at the Fe site in comparison to that in the FM state⁷. The magnetovolume effect connected to this reduction of Fe moment in the FDLM state was the reason behind the invar anomaly^{7,9}. To explore this aspect, in Fig. 3, we show the variation of the magnetic moment at the Fe site with compression for the FM, the AFM and the FDLM states. The results suggest that the Fe moments are extremely localized and there is hardly any deviation of the Fe local moment across the magnetic orders. All these observations, particularly regarding the behavior of structural and magnetic properties in the FM and the FDLM states, suggest that the experimentally observed features under pressure in Pd₃Fe are not due to a transi-

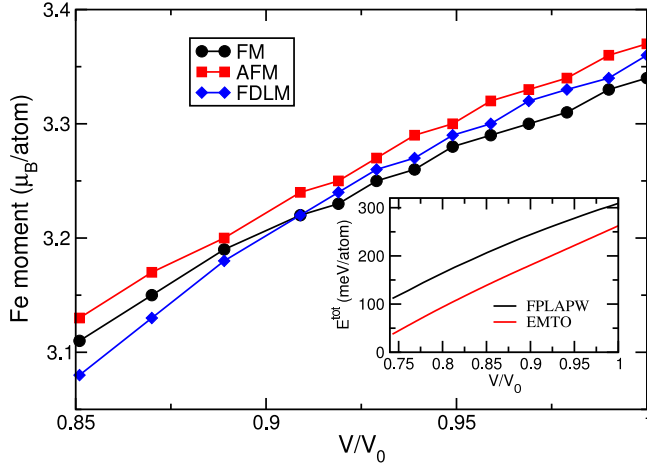


FIG. 3. (Color online) Local moments of Fe for FM, AFM and FDLM states as a function of compression computed by the EMTO-CPA method. (Inset) Total energy of LS state in meV per atom with respect to FM state as a function of compression computed by the FP-LAPW and the EMTO methods.

tion from the FM to a paramagnetic(FDLM) state. Also, we show a comparison between the relative total energies obtained in EMTO and FPLAPW methods in the inset of Fig. 3. In both methods, FM state has energy lower than that of LS state and the trend is similar as a function of compression. In Table I, we have also presented results on the equilibrium lattice constant and the bulk modulus for a low-spin(LS) state. The calculations for this state was done by keeping the spins collinear but by fixing the total magnetic moment as $0.01\mu_B$. The consideration of such a state was part of the attempt to search for a low volume low spin state which may be related to the explanation of the anomalies observed experimentally. The results suggest that the equilibrium volume of this LS state is significantly lower than the FM state and the bulk modulus considerably higher. In Fig. 4, we plot the pressure-volume relations computed by both EMTO and FP-LAPW methods. The results show a striking agreement between the experiment and the theory, both qualitatively, as well as quantitatively when one considers only the FM and the LS states. The pressure-volume relation for AFM state is also shown for comparison. It appears that the desired anomalous reduction in volume between 10-15 GPa can be explained by a transition from FM to LS state. However, upon calculating the total energy of the LS state we find that the LS state is not stable in comparison to the FM state in the desired pressure regime as shown in Fig. 4. In fact, the energy of the LS state is more than 100 meV /atom higher than the FM state around the compression (inset of Fig. 3) where the anomaly is observed and that it becomes sta-

TABLE I. The equilibrium(zero pressure) lattice constants a_0 in Å and bulk modulus B_0 in GPa for different magnetic states computed by different electronic structure methods.

Magnetic state	EMTO-CPA		FP-LAPW		Ref. 12	
	a_0	B_0	a_0	B_0	a_0	B_0
FM	3.888	204.8	3.794	216.7	3.802	216.8
AFM	3.886	202.6	3.792	218.8	3.798	216.4
LS	3.850	229.0	3.756	242.3	3.760	242.6
FDLM	3.887	206.1	—	—	—	—

ble only at a much greater compression than the FDLM state. Fig. 4 suggests that this qualitative feature is independent of the method of calculation used. This is also reported in Ref. 12. Thus the excellent agreement between the theory and the experimental pressure-volume relations can be purely fortuitous and can not be used as a viable explanation of the anomalies.

In order to resolve the observed discrepancy between the theoretical and experimental results, we next consider the following two possibilities: (i) upon application of pressure, the system does not make a transition from FM to a FDLM state but to a partially spin disordered state (PDLM) and (ii) upon application of pressure, the system may not retain the perfect chemical order, instead the system may tend to be partially ordered or fully disordered.

To check the first possibility, we have calculated the total energies of the various PDLM states with $n_{red} = \frac{n_+^{Fe}}{n_{total}^{Fe}}$ being equal to 0.6, 0.7, 0.8 and 0.9 where n_+^{Fe} and n_{total}^{Fe} are the number of spin-up Fe atoms and the total number of Fe atoms ($n_+^{Fe} + n_-^{Fe}$) respectively, n_-^{Fe} being the number of spin-down Fe atoms. The FDLM state is represented by $n_{red} = 0.5$. In Fig. 5, we present the total energies of these spin disordered states relative to the total energy of the FM state as a function of compression. The results suggest that none of the PDLM states is energetically lower than the FM state for any value of volume compression. Interestingly, one may observe that for $V_{red} \leq 0.75$, the difference in energies between the PDLM states with different n_{red} values are very close in energy. As clear from Fig. 1, this is the volume region, where EMTO-CPA should yield a FM-FDLM transition. This suggests that the transition may not occur through a FDLM state but a combination of PDLM states with different degrees of spin-disorder.

The second possibility as described above is explored by calculating total energies for partial chemical order. The fully ordered Pd_3Fe has a Cu_3Au structure with Fe on Au(I) sites and Pd on Cu(II) sites. In the partially ordered states, Pd antisites are introduced in the Fe (I) sites and the remaining Fe atoms are distributed on Pd (II) sites. In order to describe the degree of chemical order, the renormalized chemical long-range-order (LRO)

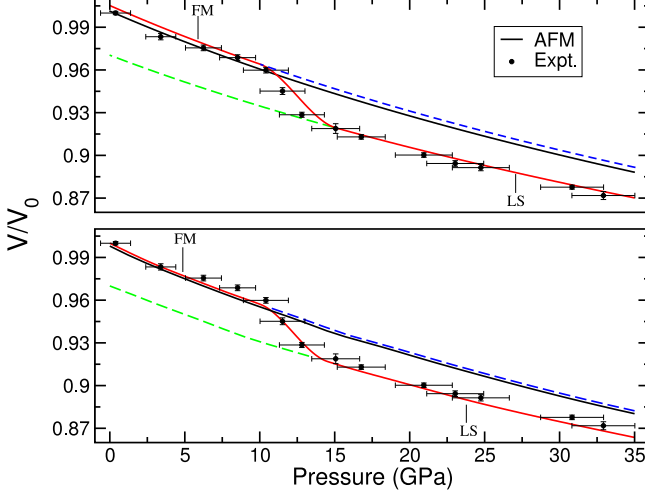


FIG. 4. (Color online) Pressure-volume relations for Pd_3Fe computed by the FP-LAPW method (top panel) and the EMT method (bottom panel). Results of FM (blue dashed), AFM (black) and LS (green dashed) states are shown in the plot. Experimental results (red line with error bars) are included for comparison.

parameter is defined in the usual way for site I as

$$S = \frac{c(\text{Pd}) - c^I(\text{Pd})}{c(\text{Pd})}, \quad (2)$$

where $c(\text{Pd})$ is total concentration of Pd in the alloy and $c^I(\text{Pd})$ is a concentration of Pd atoms on Fe site I. Thus, $S = 0$ corresponds to the fully disordered alloy and $S = 1$ corresponds to the fully ordered one. In Figs. 6 and 7, we show the results of total energy calculations for FM and various DLM states for $S = 0.5$ and $S = 0$ respectively. The first noteworthy outcome of these calculations is that the equilibrium lattice constants do not change significantly with the degree of chemical order. The lattice constants for $S = 0.5$ is 3.891 \AA and that for $S = 0$ is 3.892 \AA and thus hardly differ with that for $S = 1$ given in Table I. The equilibrium bulk modulus for $S = 0.5$ is 203.9 GPa and that for $S = 0$ is 199.5 GPa , once again showing a non-significant deviation from the value obtained for $S = 1$ (Table I). We observe the same trends for various DLM states as well. As was observed in case of $S = 1$, no signature of volume magneto-striction is observed for the partially disordered and fully disordered states. The results shown in Figs. 6 and 7 suggest that same trends in relative stabilities of PDLM and FM states as observed in Fig. 5 are preserved. With increasing degree of disorder, the energy differences between $n_{\text{red}} = 0.8$ and $n_{\text{red}} = 0.9$ PDLM states for the compression range $V_{\text{red}} = 0.9 - 0.85$, in fact increase in comparison to the fully ordered state, suggesting that the possibility of realizing a mixed state comprising of different PDLM states in this compression range decreases. In summary, the presence of both chemical disorder and

various degrees of spin disorder is not likely when one approaches the volume where the FM-FDLM transition takes place.

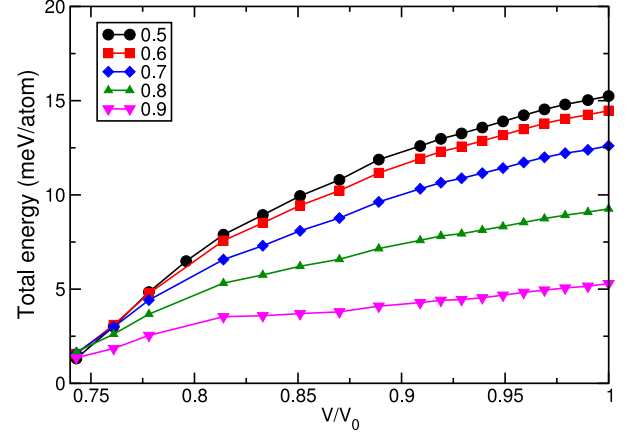


FIG. 5. (Color online) Variation of the total energies for various PDLM states as a function of compression for fully ordered ($S = 1$) Pd_3Fe . Different PDLM states are marked by the corresponding n_{red} values. The energies are measured relative to the energy of the FM configuration.

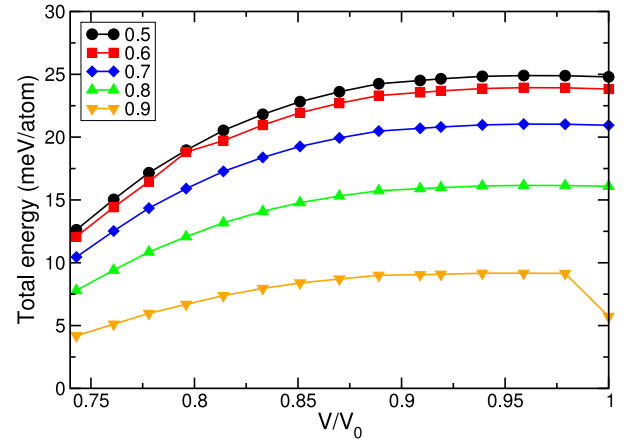


FIG. 6. (Color online) Same as in Fig. 5 but for $S = 0.5$, characterizing a partially chemical disordered state.

These results, therefore, indicate that the degree of chemical order and the degree of spin disorder do not provide us any indication towards a transition from high-volume high-spin state to a low-volume low-spin state in Pd_3Fe under pressure. However, the results presented so far were based upon collinear magnetic configurations. It has been argued that the invar anomaly in $\text{Fe}_{0.64}\text{Ni}_{0.36}$

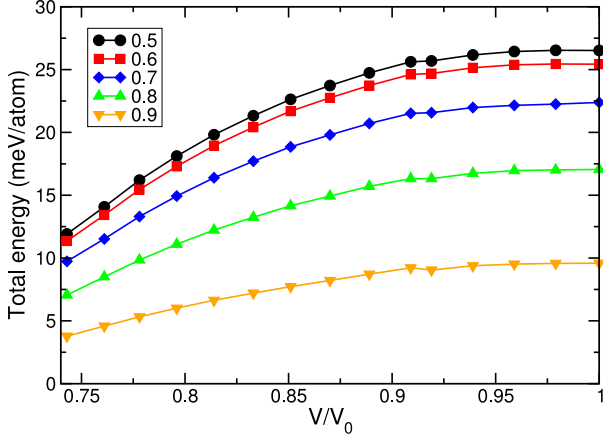


FIG. 7. (Color online) Same as in Fig. 5 but for $S = 0$, characterizing a completely disordered state.

alloys is related to the transition from collinear high spin state to noncollinear ones⁵. It is to be noted that the invar anomaly accompanied by the anomaly in the pressure-volume relation and in the variation of bulk modulus has been experimentally observed for both ambient and high pressures for various compositions, including compositions with low Fe concentrations¹¹.

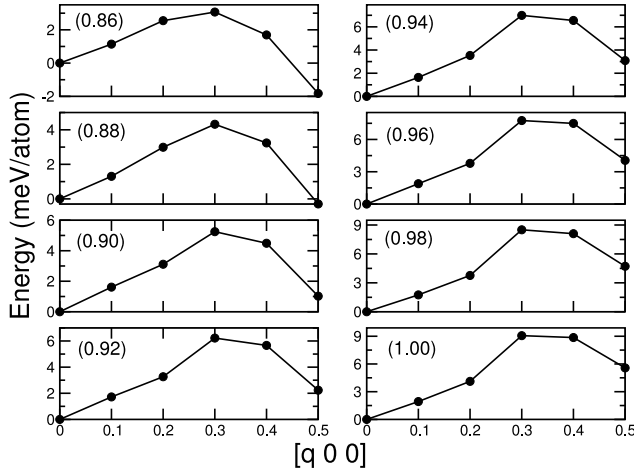


FIG. 8. Total energy as a function of spiral vector \mathbf{q} in units of $2\pi/a$ along $[\mathbf{q}00]$ direction for different compressions. In the parentheses, the values of V_{red} are shown.

Following this idea, we study the spiral magnetic states in Pd_3Fe . Specifically, we look for the possibility of non-collinear ordering by studying the energetics of spiral configurations. The total energy of the system is calculated as a function of the spiral wave vector \mathbf{q} for different

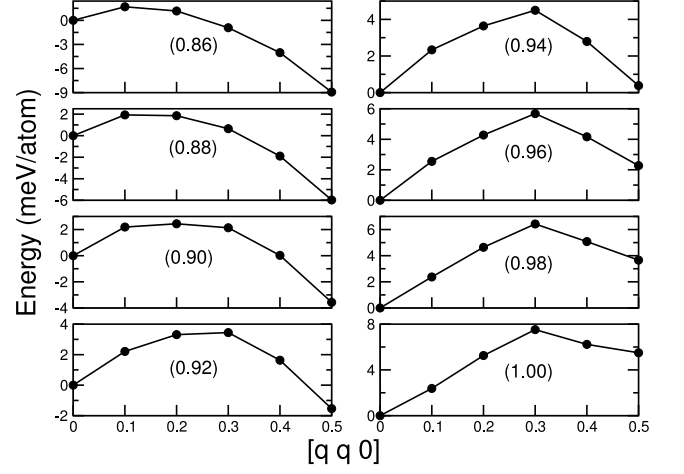


FIG. 9. Same as in Fig. 8 but for \mathbf{q} along $[\mathbf{q}\mathbf{q}0]$ direction.

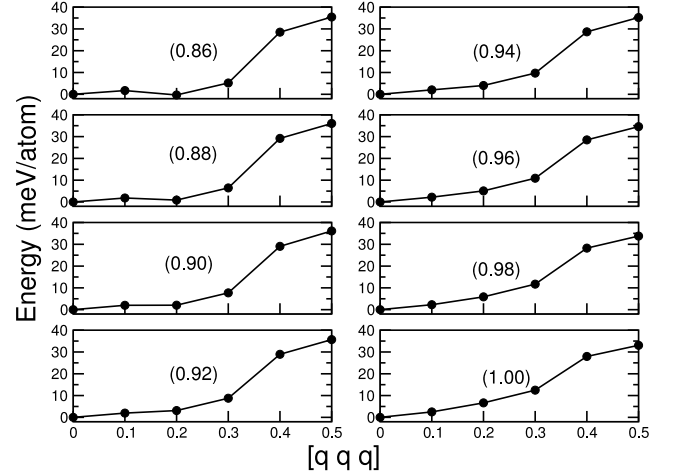


FIG. 10. Same as in Fig. 8 but for \mathbf{q} along $[\mathbf{q}\mathbf{q}\mathbf{q}]$ direction.

values of the compression V_{red} . In Figs. 8, 9 and 10, we present the results for the energetics along the high-symmetry directions $[100]$, $[110]$ and $[111]$ respectively for different compressions. Polesya *et al.*³⁰ have reported the spin spiral calculations for both ordered and disordered Pd_3Fe under ambient conditions. Our calculated results along $[100]$ direction for $V_{red} = 1.00$ are very similar to their data. The behavior of the spin spiral curve is explained in terms of the induced moment on Pd sites. Also, the reduction of Pd moment along the $[100]$ direction (data not shown here) is similar in both studies.

The analysis of the $[100]$ and $[110]$ spin spirals show that along the $[110]$ direction, there is a tendency towards the stabilization of the $[0.5\ 0.5\ 0]$ spin spiral with respect to the $[000]$ one starting from $V_{red} = 0.96$, making it lower in energy than $[000]$ one at $V_{red} = 0.92$. This

is consistent with the results of the collinear calculations shown in Fig. 1 where the AFM state becomes energetically stable than the FM around $V_{red} = 0.9$. Although, no incommensurate spin wave was found to be the lowest in energy, the energy of the $[0.4\ 0\ 0]$ spin spiral also started to decrease significantly from $V_{red} = 0.96$, finally producing a total energy lower than the FM phase ($\mathbf{q}=0\ 0\ 0$) for $V_{red} = 0.9$. Further compression resulted in the complete stabilization of various incommensurate phases over the FM phase. Analysis for $[q\ 0\ 0]$ spin spirals suggest that although no incommensurate phase or the AFM phase ($q=0.5$) is lower in energy than the FM phase ($q=0$) upto $V_{red} = 0.92$, the energy of the spirals for $q \geq 0.4$ starts decreasing continuously and at $V_{red} = 0.9$, they are within 4 meV per atom in energy to the FM state. For $[111]$ direction, we do not see any sign of stabilization of any incommensurate or AFM phase ($\mathbf{q}=0.5\ 0.5\ 0.5$) with respect to FM phase. However, the energies for $q \leq 0.2$, are less than 5 meV per atom with respect to that in the FM phase.

The following picture emerges from the assimilation of all the results on collinear magnetic states and spin spirals: first, the anomaly observed in Pd_3Fe under pressure is not a simple effect of transition from high volume FM state to a low volume paramagnetic or any low spin collinear state, and second, for the range of compression, where the anomaly is seen, there is a close competition between the FM, the AFM and other incommensurate states. This can be interpreted from the results presented in Fig. 1 and Figs. 8-10. This close competition points to the fact that the tendency of the system is to drift from a collinear high spin state to increasingly noncollinear states as a function of increasing pressure. The anomaly in the pressure-volume relation and the anomaly in the bulk modulus for different compressions, observed experimentally, act as a confirmation to this interpretation. This similar anomaly observed in $\text{Fe}_{0.65}\text{Ni}_{0.35}$ at ambient pressure⁵ and for $\text{Fe}_{0.20}\text{Ni}_{0.80}$ at finite pressures¹¹ was explained by the transition from FM to noncollinear states.

IV. CONCLUSIONS

We have performed extensive first-principles calculations on different magnetic phases of Pd_3Fe under external pressure to understand the invar related pressure-volume anomaly in a recent experiment on Pd_3Fe . The results are analyzed on the basis of relative stability of various magnetic phases as a function of compression. Contrary to the conjecture made in Ref. 12, we find that the experimentally observed invar anomaly in the pressure-volume relations and bulk modulus, can not be explained based upon either the destabilization of the equilibrium FM phase to a collinear low-spin phase or to a paramagnetic or partially spin disordered state under application of pressure. Non-collinear calculations with spin spirals also could not resolve the issue by stabilization of any incommensurate excitation under compression. However, our results suggest that in the pressure range where the anomaly is observed in experiments, the FM, AFM and some incommensurate magnetic phases compete closely, indicating that the collinear magnetic structure may be destabilized under external pressure, making the transition to non-collinear structures by the anomalous reduction of volume and increase in bulk modulus as has been observed earlier in other systems. A final resolution on this issue can be made by first-principles calculations on complete non-collinear magnetic structures as a function of pressure. This will be addressed in a future communication.

ACKNOWLEDGMENTS

BS acknowledges Göran Gustafssons Stiftelse and Swedish Research Council (VR) for financial support and Swedish National Infrastructure for Computing (SNIC) for granting computer time. BD acknowledges CSIR, India for financial support under the Grant-F. No. 09/731 (0049)/2007-EMR-I. BS is thankful to Lars Nordström for useful discussions.

* For correspondence: Biplab.Sanyal@physics.uu.se

¹ *Ferromagnetic Materials*, edited by P. Wohlfarth and K. H. J. Buschow (North-Holland, Amsterdam, 1980-1993), Vols. 1-7.

² E. F. Wassermann, in *Ferromagnetic Materials*, edited by P. Wohlfarth and K. H. J. Buschow (North-Holland, Amsterdam, 1990), Vol. 6.

³ M. Shiga, in *Materials Science and Technology*, edited by R. W. Cahn, P. Haasen and E. J. Kramer (VCH, Weinheim, 1994), Vol. 3B, Chap. 10, p. 159.

⁴ E. F. Wassermann and M. Acet, in *Magnetism and structure in Functional Materials*, Springer series in Materials Science Vol. 79, edited by A. Planes, L. Manosa and A. Saxena (Springer, Berlin, 2005), p. 177.

⁵ M. van Schilfgaarde, I. A. Abrikosov and B. Johansson, *Nature* **400**, 46 (1999).

⁶ C. E. Guillaume, *Acad. Sci. Paris* **125**, 235 (1897).

⁷ S. Khemlevskiy, A. V. Ruban, Y. Kakehashi, P. Mohn and B. Johansson, *Phys. Rev. B* **72**, 064510 (2005).

⁸ S. Khemlevskiy, I. Turek and P. Mohn, *Phys. Rev. Lett.* **91**, 037201 (2003).

⁹ S. Khemlevskiy, and P. Mohn, *Phys. Rev. B* **69**, 140404(R) (2004).

¹⁰ B. Sanyal and S.K. Bose, *Phys. Rev. B* **62**, 12730 (2000); K. Lagarec, D. G. Rancourt, S. K. Bose, B. Sanyal and R. A. Dunlap, *J. Magn. Mater.* **236**, 107 (2001).

¹¹ L. Dubrovinsky, N. Dubrovinskaya, I. A. Abrikosov, M. Vennstrom, F. Westman, S. Carlson, M. V. Schilfgaarde and B. Johansson, *Phys. Rev. Lett.* **86**, 4851 (2001).

- ¹² M. L. Winterrose, M. S. Lucas, A. F. Yue, I. Halevy, L. Mauger, J.A.Munoz, J. Hu, M. Lerche and B. Fultz, Phys. Rev. Lett. **102**, 237202 (2009).
- ¹³ S. Khmelevskyi and P. Mohn, Phys. Rev. B **68**, 214412 (2003).
- ¹⁴ P. Hohenberg and W. Kohn, Phys. Rev. B **136**, 864 (1964).
- ¹⁵ W. Kohn and L. J. Sham, Phys. Rev. A **140**, 1133 (1965).
- ¹⁶ B. L. Gyorffy, A. J. Pindor, J. B. Staunton, G. M. Stocks and H. Winter, J. Phys. F: Met. Phys. **15**, 1387 (1985); J.B.Staunton, D. D. Johnson and B. L. Gyorffy, J. Appl. Phys. **61**, 3693 (1987).
- ¹⁷ L. Vitos, Phys. Rev. B **64**, 014107 (2001).
- ¹⁸ L. Vitos, I. A. Abrikosov and B. Johansson, Phys. Rev. Lett. **87**, 156401 (2001).
- ¹⁹ L. Vitos, H. L. Skriver, B. Johansson and J. Kollar, Comp. Mat. Sci. **18**, 24 (2000).
- ²⁰ D. W. Taylor, Phys. Rev. **156**, 1017 (1967).
- ²¹ E. Wimmer, H. Krakauer, M. Weinert and A. J. Freeman, Phys. Rev. B **24**, 864 (1981).
- ²² ELK code, <http://elk.sourceforge.net/>
- ²³ L. Nordström and D. J. Singh, Phys. Rev. Lett. **76**, 4420 (1996).
- ²⁴ L. Nordström and A. Mavromas, Europhys. Lett. **49**, 775 (2000).
- ²⁵ J. P. Perdew in *Electronic structure of solids*, edited by P. Ziesche and H. Eschrig (Akademic Verlag, Berlin, 1991) pg. 11.
- ²⁶ L. Vitos, *Computational Quantum Mechanics for Materials Engineers*, Springer-Verlag, London, 2007.
- ²⁷ M. Methfessel and A. T. Paxton, Phys. Rev. B **40**, 3616 (1989).
- ²⁸ R. J. Weiss, Proc. Phys. Soc. **82**, 281 (1963).
- ²⁹ D. M. K. Paul, P. W. Mitchell and S. A. Higgins, J. Magn. Mater. **54-57**, 1171 (1986).
- ³⁰ S. Polesya, S. Mankovsky, O. Sipr, W. Meindl, C. Strunk and H. Ebert, Phys. Rev. B **82**, 214409 (2010).